5-2016

The Skin Disease Mutation Cx31L209F Induces a Calcium- and Cobalt-Sensitive Leak Current Across the Plasma Membrane

Husain A. Bneed
husain.awad@yahoo.com

Advisor
I. Martha Skerrett, Ph.D., Associate Professor and Chair of Biology
First Reader
I. Martha Skerrett, Ph.D., Associate Professor and Chair of Biology
Second Reader
Gary W. Pettibone, Ph.D., Professor of Biology
Third Reader
Derek L. Beahm, Ph.D., Research Assistant Professor of Biology
Department Chair
I. Martha Skerrett, Ph.D., Associate Professor and Chair of Biology

The Skin Disease Mutation Cx31L209F Induces a Calcium- and Cobalt-Sensitive Leak Current across the Plasma Membrane

by

Husain Awad Bneed

An Abstract of a Thesis

in

Biology

Submitted in Partial Fulfillment

of the Requirements

for the Degree of

Master of Arts

May 2016

Buffalo State College

State University of New York

Department of Biology

ABSTRACT OF THESIS

The Skin Disease Mutation Cx31L209F Induces a Calcium- and Cobalt-Sensitive Leak Current across the Plasma Membrane

Gap junctions are essential to the function of multicellular animals, which require a high degree of coordination between cells. The functions of gap junctions are highly diverse and include exchange of metabolites and electrical signals between cells, as well as functions apparently unrelated to intercellular communication. In vertebrates, gap junctions are comprised of connexin proteins and over 20 connexins have been identified in humans. Each connexin is named according to its predicted molecular weight, for instance connexin31 (Cx31) has a predicted molecular weight of 31 KDa. Mutations in connexin genes cause a variety of disorders depending on the connexin protein affected. Cx31 is one of the gap junction proteins expressed in skin and the inner ear. Some point mutations cause a rare skin disease termed erythrokeratodermia variabilis (EKV) whereas other mutations cause non-syndromic hearing loss (NSHL). The main goal of this project was to create, express and study Cx31L209F, a hereditary skin disease mutation which occurs in the fourth transmembrane domain. Other mutations (S26T, C86S and L135V) were also briefly studied. The L209F mutant induced large membrane currents and compromised the health of single cells suggesting that aberrant hemichannel behavior may underlie the disease pathology. Cell death in L209F-expressing cells was rescued by the addition of 2 mM calcium or 1 mM cobalt, conditions known to block hemichannel function. Two of the other mutations S26T, and L135V appeared to form gap junctions with altered gating properties.

Buffalo State College
State University of New York
Department of Biology

The Skin Disease Mutation Cx31L209F Induces a Calcium- and Cobalt-Sensitive Leak Current across the Cell Membrane

A Thesis in
Biology
By

Husain Awad Bneed

Submitted in Partial Fullfillment
Of the Requirements for the Degree of

Master of Arts

May 2016

Approved By:

I. Martha Skerrett, Ph.D.
Thesis Advisor and Chair of the Committee

I. Martha Skerrett, Ph.D.
Associate Professor and Chair of Biology

Kevin Railey, Ph.D.
Dean of the Graduate School
Associate Provost

Thesis Committee

I. Martha Skerrett, Ph.D.
Associate Professor of Biology

Gary W. Pettibone, Ph.D.
Professor of Biology

Derek L. Beahm, Ph.D.
Research Assistant Professor of Biology

Acknowledgements

I would like to express my sincere appreciation to my great advisor Dr. Martha Skerrett for everything; support, advice, encouragement and supervision for the last two years. Without her, this work would have never been finished.

To the Higher Committee for Education Development in Iraq (HCED), I would like to say thank you for giving me this great opportunity to finish my higher education in the U.S. and supporting me throughout my study.

Also I would like to thank my committee members, Dr. Derek Beahm and Dr. Gary Pettibone for their advice about this research.

I would like to thank all the staff in the biology department at Buffalo State for their support and encouragement. Also I want to thank all the graduate students in Dr. Skerrett's lab for their help.

In the end and from deep of my heart, I would like to thank my father, mother, brothers, sisters and my lovely wife, Seemaa. I am grateful to everyone of you. You are my source of my inspiration. With your support, I achieved my goal and got my degree successfully.

Husian Awad Bneed

TABLE OF CONTENTS

LIST OF FIGURES

Introduction

Gap junctions are specialized membrane structures that provide an intercellular pathway for the propagation of signals and diffusion of ions and metabolites between cells. They also have functions that are unrelated to transport such as signaling (Alberts *et al*., 2005). The proteins that form gap junctions in vertebrates differ from those that form gap junctions in invertebrates. In vertebrates, gap junctions are formed by connexins, whereas invertebrate gap junction proteins are called innexins (Phelan 2005).

Gap Junction Structure

Connexin proteins are the major components of vertebrate gap junction channels and are arranged to form aqueous pores that connect the cytoplasm of two cells, allowing the transfer of ions and small molecules (Saez *et al*., 2005). Each connexin protein has four transmembrane domains, cytoplasmic amino- and carboxyl termini and two extracellular loops (Figure 1a). The sequence and structure of the extracellular loops are important determinants of docking interactions. Six connexin proteins assemble to form a connexon which is also known as a hemichannel. Each gap junction channel is composed of two connexons, which connect or "dock" in the extracellular space (Figure 1b). Connexons that are composed of the same connexins are referred to as homomeric, while connexons of different connexins are called heteromeric. Additionally, gap junction channels formed from the same two connexons are referred to as homotypic, whereas gap junctions formed from different connexons are referred to heterotypic (Figure 2a). All of these interactions create a broad range of properties in the resulting gap junction channels (Goodenough and Paul, 2009).

The Connexin Family of Proteins

In humans, over 20 different connexin proteins are expressed and each is named according to its molecular weight (Scott and Kelsell, 2011). Their expression patterns are cell specific and are also overlapping. Connexin interactions occur when multiple connexins are expressed in the same cell or in adjacent communicating cells. Interactions may occur in the endoplasmic reticulum, as the connexin is being trafficked through the golgi apparatus or when connexons dock to form intercellular channels (Figure 2b). Like most integral membrane proteins, connexins are co-translationally inserted into the ER (endoplasmic reticulum). Properly folded connexins are expected to pass through the ER-Golgi intermediate compartment (ERGIC) prior to entering the cis-Golgi network (Figure 2b). Several studies have revealed that connexins pass through the Golgi apparatus (Musil and Goodenough, 1993). However, other studies have reported that Cx26 can reach the cell surface via a Golgi-independent pathway (Evans *et al*., 1999).

Connexin-Related Diseases

Connexin mutations cause a variety of disorders depending on the connexin protein affected (Scott and Kelsell, 2011). Connexin31 (Cx31), the focus of this study, is expressed in skin, inner ear (Figure 3a and b) and peripheral nerves. Mutations are most commonly associated with skin disease but may also cause deafness and/or neuropathy in humans (Richard *et al*., 1998; Scott and Kelsell, 2011). This indicates that Cx31 has a role in epidermal differentiation, auditory and neuronal function (Unsworth *et al.*, 2007). Furthermore, mutations associated with the same condition may be inherited in an autosomal dominant pattern (eg. the skin disease mutation Cx31R42P, Richard *et al*.,

1998) or a recessive pattern (eg. the skin disease mutation Cx31 L34P, Gottfried *et al.,* 2002).

Mutations associated with skin disorders specifically cause erythrokeratodermia variabilis (EKV) which is classified as a rare skin disease causing abnormal and often dangerous skin thickening known as hyperkeratosis (Richard *et al*., 1998; Scott and Kelsell, 2011). Mutations that affect the ear cause non-syndromic hearing loss (NSHL) (Laird, 2006). NSHL appears to occur when intercellular communication within the cochlea is disrupted, altering potassium distribution (Kikuchi *et al.,* 2000).

Interestingly, some Cx31mutations cause only skin disease, some cause only deafness, while others have widespread effects. For instance, the G12R mutation specifically causes EKV (Itin *et al*., 1998; Diestel *et al*., 2002) , the mutation V43M causes deafness (Oh *et al.,* 2013) and the mutation Del66D is associated with sensorineural hearing loss and peripheral neuropathy (López-Bigas *et al*., 2001). It is unlikely that these differences are based solely on the severity of the mutation, and it has been postulated that the location of a mutation in relation to specific protein domains might be important. For instance, it was postulated that mutations within the extracellular loops are more likely to cause skin disease (López-Bigas *et al*., 2002), while those in other parts of the protein cause deafness (Kelsell *et al.,* 1997). While this does not appear to be the case, as new mutations within other domains have been identified, it could highlight the importance of variable connexin roles in different tissue.

Understanding the consequences of a mutation requires an understanding of protein synthesis and trafficking, as well as understanding protein structure-function relationships. Connexin proteins have a half-life of a few hours and this short lifespan has

been well-documented in cultured cells and in tissue (Laird 2006). Thus, for reasons that remain unclear, connexins are pre-programmed to be continually biosynthesized and degraded. It has been suggested that the short half-life is related to a requirement for rapid regulation of coupling in response to physiological changes (Laird, 2006). The oocyte expression system will be used to assess function of Cx31 mutations in this study. The oocyte expression system is ideal for characterizing properties of gap junction proteins that traffic to the membrane and form channels with aberrant properties. Ideally it is used in combination with studies of trafficking and oligomerization, particularly when a mutation fails to form channels.

Analysis of Cx31L209F and Other Mutations that Cause Skin Disease

The epidermis of the skin is composed primarily of keratinocytes which undergo differentiation, leading to the formation of stratum corneum which forms the skin barrier. Cx31 is highly expressed in the stratum granulosum which is part of the upper differentiating layer of the epidermis (Di *et al*., 2001). While the majority of experiments focused on L209F, several other mutations were also studied including S26T, L135V and C86S. The locations of these mutations are highlighted in Figure 1a and a brief summary of the literature related to their identification and characterization is summarized below.

Cx31S26T is a poorly studied mutation associated with EKV (Richard *et al.*, 2000) listed on the Connexin-Deafness Homepage (*http://www.crg.es/deafness)* under "*Connexins Causing Other Diseases*". It involves substitution of threonine

for serine at position 26 within the first transmembrane domain. There does not appear to be any literature related to its expression and characterization.

Cx31C86S was one of the first Cx31 mutations associated with EKV (Richard *et al.,* 1998). It involves substitution of serine for cysteine at position 86 within the second transmembrane domain. When it was expressed in Hela cells it appeared to induce cell death (He *et al*., 2005). Cell death did not appear to occur as a result of hemichannel formation. Tattersal and colleagues (2009) further identified an upregulation of the unfolded protein response (UPR) as a result of ER retention after expression of C86S in cells. By using the oocyte expression system, we aim to determine if C86S is capable of forming functional gap junction channels and if so, to further assess the properties of those channels.

Cx31L135V was identified in a family with the skin disorder EKV (Scott *et al.,* 2011). This mutation involves an amino acid substitution of valine for leucine at position 135. The residue L135 is located at the border between the cytoplasmic loop and the third transmembrane domain (Figure 1a). This dominant mutation has been expressed in mammalian cells. It appears to traffic to the plasma membrane but does not facilitate dye transfer between cells (Rouan *et al.,* 2003; Tattersall *et al.,* 2009). This suggests incorrect assembly or altered properties of the resulting gap junctions.

Cx31L209F The Cx31 mutation L209F was identified in a family with EKV and in one unrelated sporadic case (Morley *et al.,* 2005). This mutation may have structural

and/or functional significance because it occurs at a conserved phenylalanine residue at the border of the cytoplasmic carboxyl terminus and fourth transmembrane domain. (Morley *et al.*, 2005). To the best of our knowledge, the L209F mutation has not been previously expressed in oocytes or mammalian cultured cells to investigate the functional consequences of the mutation.

Expression in Xenopus Oocytes

Oocytes were extracted from *Xenopus laevis*, a frog found in South Africa. These cells are primarily used because of their large size and easiness to maintain and are considered the most convenient system to study exogenously expressed ion channels (Dascal, 1987). Gap junction channels form between oocytes when gap junction proteins are expressed and cells are paired together after removal of the vitelline layer (Werner *et al*, 1985). By coupling oocytes and measuring intercellular junctional conductance, properties of mutated gap junctions can be compared to the wild type. This study may provide insight into the ways Cx31 mutations effect human physiology and eventually allow preventative measures for treatment EKV and NSHL.

Methods

Overview

The hCx31 gene (*GJB3*), was obtained as a gift from Dr. David Kelsell (*Barts and the University College of London*). The gene was transferred to a TOPO-CT GFP vector by Shelby Rarick (*SUNY Buffalo State*). Important features of this vector include a priming site for RNA polymerase, ampicillin resistance sequences, a multiple restriction site, and a c-terminal GFP tag (Figure 4). For our studies, a stop codon was included at the end of the Cx31 sequence to prevent GFP-fusion as our goal was to characterize properties of mutants rather than study their localization. Site-directed mutagenesis was used to create the mutation L209F. The mutations S26T, C86S and L135V were created as part of a class project in BIO314 Advanced Cell Biology (*Spring 2014*).

Primer Design

To facilitate sequence-related aspects of the project, a group of programs offered through Biology Workbench (San Diego Supercomputer, SDSC) was used. The human Cx31 gene sequence *(GJB3)* was obtained through NCBI (*accession number gi_54607054*), uploaded as a nucleotide file, and using the Six Frame function of Biology Workbench, the longest Open Reading Frame (ORF) was determined. This sequence was selected and saved as a translated protein file.

In order to design primers for the mutation L209F, the Stratagene Quikchange Primer Design software (*Agilent Technologies, Santa Clara, CA*) was used. The adjustment was made at the 209th codon, originally coding for leucine, converting it to the codon for phenylalanine. Mutagenic primers were ordered from IDT (*Integrated DNA*

Technologies, Coalville, Iowa) and they were complementary to one another because each primer initiates DNA synthesis on a complementary strand of the plasmid. Forward and reverse primers (labelled L209Fa and L209Fb, respectively) were 31 nucleotides in length and had a Tm of 78.28 ^{0}C (Figure5).

Site- Directed Mutagenesis

The QuikChange method of mutagenesis was used to create the L209F mutation (*Quikchange Mutagenesis Kit, Agilent Technologies*). In the first part of the mutagenic process, PCR was used in combination with the mutagenic L209F primers to produce site-directed mutated DNA. Primers were obtained as lyophilized powder. They were reconstituted by adding 100 µl of nuclease-free water. Primers were further diluted by mixing 10 µl of primer with 90 µl of nuclease-free water immediately prior to the reaction. In order to calculate an appropriate primer concentration and volume for the mutagenesis reaction the mass of each primer was obtained from the information provided by the primer-synthesis company (IDT, Coralville Iowa). Primer L209Fa was reconstituted from a mass of 0.25 mg/ml and L209Fb from a mass of 0.28 mg/ml. The volume of each primer added to the mutagenesis reaction is shown in Figure 6. The reaction also requires 20 ng of template DNA (the plasmid containing Cx31), reaction buffer, dinucleotide triphosphates (dNTP mix), and a DNA polymerase (Quikchange Lighetning DNA Polymerase, Agilent Technologies, Santa Clara Inc). The polymerase is a high fidelity DNA polymerase that extends mutagenic primers during each PCR (Polymerase Chain Reaction) cycle. PCR is a temperature-dependent process with three key steps. The first step is denaturation at 95^{0}C, the second step in annealing at 65^{0}C, and

the final step is extension at 70^0C. These processes are facilitated through the use of a thermocycler (BIO RAD, Singapore), which is capable of accurately and quickly changing temperature and completing 18 cycles in about 90 minutes. Each cycle creates mutated Cx31 plasmid DNA using the original DNA as a template. Unlike amplifying PCR reactions, the newly synthesized daughter strands are not used as templates in subsequent cycles. In this application, the daughter strands contain nicks created adjacent to the incorporated primers.

After the mutagenic thermocycler session, 2µl of DpnI restriction enzyme was added. The DpnI restriction enzyme digests methylated DNA leaving new non-methylated mutant strands intact. In our case the Dpn-digest involved an accelerated enzyme (*Fast-Digest Dpn,* Agilent Technologies, Santa Clara Inc) and the reaction was incubated at 37^0C for 15 minutes before the DNA was stored at -20^0C for further analysis

The Dpn-digested DNA was used to transform competent cells (*XL-10 Gold Ultracompetent Cells, Agilent Technologies, Santa Clara).* Two microliters of the DpnI – treated DNA were transferred to a 14 mL tube containing 50 µl of XL-1 super competent cells. The contents were swirled gently. The reaction was then heat' pulsed for 45 seconds at 42 °C and placed back on ice for 2 minutes. About 500µl of 42^0C pre-heated nutrient broth (*SOC- 20 g/L tryptone, 5 g/L yeast extract, 4.8 g/L MgSO4, 3.6 g/L dextrose, 0.5g/L NaCl, 0.186 g/L KCl, Agilent Technologies, Santa Clara)* was then added before placing in a shaking incubator for 1 hour at 37^0C. Using a sterilized glass rod, 250µl of transformed bacteria was spread evenly on each of two plates. Plates were made with LB medium supplemented with ampicillin (10g/l tryptone, 10g/l NaCl, and 5g/l yeast extract, 100 µg/ml ampicillin) and 1% agar. The presence of ampicillin

facilitates selection of cells carrying our Cx31 plasmid. Plates and then incubated overnight at 37°C. The following day single colonies were observed and the plates were wrapped in parafilm for storage at 4 °C.

Individual colonies were transferred to about 2 ml of LB medium (10g/l tryptone, 10g/l NaCl, and 5g/l yeast extract, 100 µg/ml ampicillin). Innoculation was performed using the "flame and loop" method. This process was repeated 4 times. Incubated tubes were placed in a shaking incubator overnight at 250 RPM and 37^0C.

A glycerol stock was created for each selected colony in preparation for identification of a successful mutation. Three tubes were filled with 500µl of glycerol each and then 500µl of the three most turbid cultures was transferred to the stock tubes. These tubes were carefully labeled L209Fa, b and c to allow association of sequencing results. After being mixed, the stock tubes were stored at -80^0C.

The remaining culture was used for plasmid isolation. About 1.5 ml was centrifuged at 13,000 rpm in a table top centrifuge, the supernatant discarded and the pellet used in a Qiagen miniprep procedure using centrifugation (Qiagen Inc, Mississauga, ON). In the final step, 50 µl of plasmid DNA was eluted in the provided elution buffer. Gel electrophoresis was performed to assess the approximate concentration of plasmid DNA. Two microliters of plasmid DNA from each sample was mixed with 4 µl of loading dye then samples were loaded on a 1% agarose gel including ethidium bromide, alongside 5µl of DNA ladder to estimate concentration (*ZipRuler 2, Fermentas Inc)*. Following electrophoresis at 90 mV for 20 minutes, samples were visualized under ultraviolet light and concentration was estimated by comparing the

intensity of experimental DNA bands to the known bands in the ladder. After confirming that DNA concentration was greater than 20 ng/µl, small volumes were sent to Genscript (Piscataway, NJ) for sequence analysis. Sequencing was performed using the Sanger sequencing method with T7 primers. Biology Workbench (SDSC) was used for sequence analysis. Nucleotide sequences were downloaded from Genscript and translated using SixFrame. Successive alignment of the wtCx31 protein sequence with each mutated sequence shows altered nucleotides and sequence accuracy. All samples gave excellent sequencing through the 207^{th} codon and all contained the mutation resulting in an L209F substitution. Figure 7 shows an alignment of one of the L209F samples. The L29F substitution is noted in the last line with a box. Other than the targeted mutation, and some mismatches at the end of the sequence read, the L209F was identical to Cx31.

In Vitro Transcription

DNA was linearized with Xba1 to prepare for *in Vitro* transcription. Xba1 cuts the TOPO vector downstream of the Cx31 coding region (Figure 5). Since all three samples contained the mutation, the sample with the highest concentration of plasmid DNA and the longest sequence read was chosen. Double autoclaved microfuge tubes were used for this procedure to prevent contamination with RNase enzymes that might affect subsequent steps. Ten microliters of DNA was linearized in a reaction that included 10x reaction buffer and 2µl of fast digest Xba1 restriction enzyme. The reaction was incubated at 37^0C for 25 minutes. Following linearization**,** RNA was transcribed *in vitro* using a mMessage mMachine *in vitro* transcription kit (Applied Biosystems/Ambion, Austin TX) and recovered via LiCl precipitation method, after precipitation and

reconstitution the RNA was run on a 1% agarose gel alongside an RNA control (*RNA 250, Applied Biosystems, Austin TX*). The results are shown in Figure 8a. The RNA was then diluted to a concentration of 125 ng/µl or 68 ng/µl with nuclease-free water (Applied BiosystemsAustin TX) prior to injection. Diluted samples of the RNA are shown in Figure 8b. Given a typical injection volume of 40 nl, these concentrations result in about 5 ng and 2.5 ng of RNA per oocyte.

Expression in Xenopus Oocytes

Oocytes were surgically removed from *Xenopus laevis* females and treated with collagenase in order to remove the follicle layer. They were cleaned and digested in Oocyte Ringers 2 (OR2; 82.5 mM NaCl, 2 mM KCl, 1 mM $MgCl_2$, 5 mM HEPES, pH 7.4) and maintained in modified Barth's (MB1) solution (88 mM NaCl, 1 mM KCl, 0.41 mM $CaCl_2$, 0.82 mM $MgSO_4$, 1 mM $MgCl_2$, 0.33 mM $Ca(NO_3)_2$, 20 mM HEPES, pH 7.4) (Figure 8a). All oocytes used for gap junction studies were pre-injected with 0.1 ng of morpholino antisense oligonucleotide directed against *Xenopus* Cx38 (Gene Tools LLC, Philomath, OR). An NanojectII microinjector (*Drummond Scientific, Broomall, PA)* was used to inject the RNA.. RNA was typically injected at a final concentration of 125 ng/µl (total RNA ~ 5 ng/oocyte). For single oocyte analysis, oocytes were maintained in shallow culture dishes bathed in MB1. For gap junction studies, the vitelline layer was removed and oocytes paired in agar wells (1% agar in MB1) to allow intercellular channel formation.

For analysis of single oocytes, a two-electrode voltage clamp was used. For gap junction studies two of the same amplifiers (*Axopatch200B, Molecular Devices,*

Sunnyvale CA) were used to create a dual cell two-electrode voltage clamp. Dual cell clamping allowed us to determine junctional conductance and assess voltage-dependence of gap junction channels. One electrode senses voltage in each cell and the other injects current to clamp the voltage. The "clamp" current reflects the membrane conductance. In order to acquire and analyze our data, the programs Clampex10 and Clampfit10 (Molecular Devices, Sunnyvale CA) were used. The program Origin8 (OriginLab, Northampton, MA) was used for graphing and statistical analysis.

Results and Discussion

Hydropathy Analysis of L209F

In membrane proteins, including connexins, large, bulky amino acids tend to cluster at the boundaries of membrane-spanning domains (Mall *et al.,* 2001; Maeda *et al.,* 2009; Brennan *et al.,* 2015) and it has been postulated that inserting or substituting bulky side-chains could influence membrane topology (Brennan *et al*., 2015). Residue L209 is located near the cytoplasmic boundary of the fourth transmembrane domain suggesting that phenylalanine substitution might alter topology. Topology prediction software is readily available and using TMHMM (Krogh *et al.,* 2001, Biology Workbench, SanDiego Super Computer) we compared the predicted amino acids contributing to the fourth transmembrane domain of Cx31. It was noted that L209F did not influence topology as shown in Figure 9. In both Cx31 and L209F residues 188 through 210 are predicted to lie

within the membrane. While this predictive software does not provide definitive evidence regarding insertion of transmembrane domains, it should be noted that at least one other mutation (eg. R42P) was found to alter the predicted membrane topology providing a possible explanation for the abnormal behavior of the resulting channels (*John Lang and Daniel Abbatoy, Bio314 Class Project).*

Expression of Cx31L209F Compromises the Health of Oocytes

The main goal of oocyte expression was to determine if L209F was capable for forming gap junctions. The first attempts to express L209F in oocytes were challenging. The oocytes typically died before they could be paired and on rare occasion when they survived long enough to be paired the pairs died before we could record intercellular currents. Images of oocytes after injection (Figure 10) show the appearance of healthy versus unhealthy oocytes. Healthy oocytes maintain a clear division of pigment, with animal (dark colored) and vegetal (light colored) pigments divided by an "equator". Unhealthy oocytes typically lose the clear division of pigmentation prior to bursting and release of yolky cytoplasm.

Cx31L209F May be Capable of Forming Gap Junctions

We were able to record one set of intercellular currents from paired oocytes expressing the mutant L209F (Cx31/L209F) and it appeared that the mutant was able to form functional channels. These results are shown in Figure 11, middle row left image.

In contrast to Cx31 (top two sets of traces) the pair involving L209F did not exhibit voltage-dependent inactivation. The lack of voltage-dependence may indicate that these currents are not really representative of gap junctions. Intercellular currents that lack voltage sensitivity often reflect membrane fusion. Another issue with the traces is that both sides of the junction lack voltage sensitivity. A more typical result for a mutation that disrupted voltage sensitivity would be an asymmetric set of junctional currents with gating at least retained on the wild-type side. In summary, although L209F induced intercellular currents between oocytes, there is little evidence to suggest that gap junction channels were responsible. It is more likely that membrane fusion occurred which would be consistent with observation that oocyte health was compromised by the oocytes. Further studies of paired oocytes are needed to confirm or refute the ability of L209F to form gap junctions. These may be possible using new evidence shown below indicating that calcium and cobalt can be added to the media to enhance viability of L209F-expressing oocytes.

Two Other Cx31 Mutants form Gap Junctions with Altered Properties

Two other Cx31 mutants were expressed in oocytes and formed gap junction channels. These include L135V and S26T (Figure 11, middle row right and bottom row left respectively) which both formed gap junctions with aberrant gating properties. The voltage sensitive properties of these mutants can be compared with Cx31/Cx31 channels (top row). In both cases the mutants were paired heterotypically with wildtype Cx31 and asymmetric currents were observed. In these preliminary experiments we did not note

orientation of the paired oocyte so we cannot definitively assign specific gating properties to the mutants. However it is most likely that the oocyte displaying the voltage-dependent inactivation is the Cx31-expressing oocyte. For both mutants, one of the oocytes is expressing gap junction channels that activate (rather than inactivate) in response to voltage. This is apparent as a slight increase in outward current at higher voltages (note that this is the opposite response to wild-type connexins).

Changes in voltage sensitivity suggest that structural rearrangements have occurred within the regions of the protein responsible for sensing voltage and/or gating. For connexins in general, there is evidence that the transjunctional voltage (Vj) sensor lies within the amino terminal domain (Verselis *et al*., 1994; Harris 2001) and that gating in response to Vj occurs as a result of global rearrangements of transmembrane domains (Skerrett *et al.*, 1999; Harris 2001; Brennan *et al*., 2015). Our results suggest that S26T, may cause the channel to remain partially closed at rest, but open in response to Vj. Similar observations have been made for a number of connexin mutations including several that are associated with disease. For instance Cx26M34T is one of the most prevalent deafness mutations and it also induces a reversal in gating response (Skerrett *et al.*, 2004). The mutation L135V has a similar but less dramatic effect on channel properties. At rest, the channels appear to be open but conductance increases with higher Vj. Further studies are required to confirm the results that Cx31S26T and Cx31L135V form gap junction channels with aberrant properties.

Unusual Voltage-Dependent Gating of Cx31

There is very little published information related to electrophysiological analysis of Cx31 (Abrams *et al*., 2006) and nothing published so far regarding expression of Cx31 in oocytes. While analyzing the behavior of wtCx31 in oocyte pairs it was noted that the responses in my experiments (Figure 11) are very similar to those of other students (Shelby Rarick, Honors Thesis; Shahd Kadhim, MA Thesis) that have expressed Cx31 in oocytes. Connexins vary greatly in their sensitivity to Vj, and Cx31 appears to be one of the least sensitive (Abrams *et al.*, 2006; Harris, 2001). Direct comparison of the time-course of inactivation are possible by fitting an exponential curve to the data and obtaining a time constant of inactivation at a particular voltage. This analysis is ongoing and requires additional data that includes longer pulse lengths than those employed in this study. An interesting observation made while attempting to record longer pulses revealed that longer pulses (eg. 5- 20 seconds) induced subsequent decreases in conductance. This suggests that the channels are not fully recovering after they close in response to voltage. Similar observations were made by Shahd Kadhim (2015) while working on her Master's thesis in our lab. When high Vj was applied, even after recovery times up to 5 minutes, gap junction conductance did not recover. This is very unusual as gap junction channels composed of most connexins gate to the maximum extent within a few seconds and then recover fully within seconds. A detailed analysis of Vj sensitivity in wtCx31 is ongoing.

In this study Cx31 Vj-recovery was briefly investigated using a pulse protocol involving repeated pulses to 100 mV, followed by a variable recovery period prior to a Vj pulse to 100 mV in the opposite polarity. If the channels recover between the 100 and -100 mV pulses the magnitude of the current should be the same in the recovery pulse as

in the original pulse. A similar pulse protocol is used to test recovery from inactivation in voltage gated sodium and potassium channels (Landowne, 2006). When this pulse protocol was applied to Cx31 (Figure 11 bottom right) with each pulse to 100 mV the recovery current became smaller regardless of the time allowed for recovery. This suggests that Cx31 may possess a gating mechanism that is unique amongst the connexins and identifies an added consideration for assessing voltage sensitivity of Cx31 mutants.

Expression of Cx31L209F Causes Leaky Membranes

In order to further study the mechanism by which expression of L209F reduced oocyte viability we measured membrane currents in single oocytes expressing L209F. The results are shown in Figure 12. Single oocyte voltage clamp was used to pulse oocytes between -160 mV and 60 mV. Expression of Cx31 caused very little change in membrane properties from that of the negative control (compare filled squares and filled triangles). The "oligo" control involved injection of an antisense morpholino, pre-injected to reduce expression of endogenous XeCx38. All oocytes receive this "oligo" injection prior to injection of connexin RNA. Figure 12 also shows currents induced by two other mutants C86S and L135V which cause very mild changes in the current levels. Work by future students will focus on expression of these mutants in other batches of oocytes and the significance of these minor changes in current will be assessed. However, L209F induces very large leak currents. These currents saturate the capability of the voltage clamp outside the range of -40 to +40 mV producing the S-shaped current versus voltage

curve. Most important is the region where current is accurately reflected (-40 mV to 40 mV) where L209F is strikingly different than Cx31 or other mutants.

The observation that L209F induces leak currents in oocytes is indicative of altered regulation of hemichannel (connexon) activity. Prior to docking, connexons must be regulated to prevent ions and metabolites from leaking across the membrane of the cell prior to gap junction formation. This is in part carried out by a "loop gate" at the extracellular end of the first transmembrane domain (Harris 2001; Verselis *et al.*, 2009). Altered hemichannel behavior is unfolding as a key mechanism in connexin-associated disease (Martin and van Steensel, 2015; Lilly *et al.*, 2016). In particular several of the connexins expressed in skin and ear have hereditary mutations associated with disease and aberrant hemichannel activity (Garcia *et al*., 2015; Lilly *et al.*, 2016). This is the first observation that Cx31L209F is a mutation that induces aberrant hemichannel behavior and is a plausible explanation for the effects of L209F in terms of skin disease. Targeting aberrant hemichannel activity with blockers may provide therapeutic relief for symptoms of skin disease.

Further investigation of L209F-expression in single oocytes.

To better understand aspects of L209F-mediated cell death we investigated the effect of RNA concentration and the time-course of cell death. As expected, there was a strong correlation between the amount of RNA injected and the viability of oocytes one day post-injection. For all the experiments described thus far, oocytes were injected with about 5 ng of RNA (injection volume = 41 nl, RNA concentration ≈ 125 ng/µl), a quantity that is thought to be optimal for the expression of wtCx31.

Figure 13 summarizes the association between RNA levels and cell viability for one batch of oocytes. RNA dilutions were made so that full strength equaled 125 ng/µl, ½ strength equaled 68 ng/µl and ¼ strength equaled 34 ng/µl. Cx31 was tested at full and half strength. L209F was tested at full, one-half and one-quarter strength. For this particular batch about 85% of uninjected oocytes survived, about 65% of Cx31 (full-strength) and about 52% of L209F (full-strength) survived. Viability increased to almost control levels in the ½ strength Cx31 group and the ¼ strength L209F group. Although survival rates varied between batches of oocytes similar patterns were observed in other groups of cells.

The correlation between RNA quantity and survival is consistent with a hemichannel-induced mechanism of cell death. A hemichannel-related mechanism of cell death would also be consistent with more rapid decline in oocyte health when higher numbers of channels are formed. The time-course of cell death is plotted in Figure 14 for oocytes injected with varying amounts of L209F RNA. Oocytes injected with RNA encoding Cx31 survived for at least 48 hours after injection (open circles). In this wildtype group, even after 66 hours almost half of the oocytes were still alive. In contrast, less than 10% of oocytes injected with L209F (125 ng/µl) were alive after 40 hours. Overall there was a strong correlation between the amount of L209F RNA injected and the survival of the oocytes.

Oocytes expressing L209F are rescued by calcium and cobalt

Some connexins that naturally form hemichannels (eg. Cx50) are regulated by external calcium concentration (Harris 2001; Ebihara 2003). Mild increases, for instance

1 mM, in external calcium reduce the magnitude of connexin-dependent membrane currents (Harris 2001). For this reason, regulation of membrane currents by calcium is often viewed as evidence of hemichannel behavior, most often to investigate the behavior of wildtype connexins (Harris, 2001). Less frequently, cobalt is also used (Malchow *et al.*, 1993). Both calcium (2 mM) and cobalt (1 mM) enhanced the survival of L209F-expressing oocytes. Both ions were added to the MB1 solution as chloride salts immediately after oocytes were injected with connexin RNA. Aboout 40 hours after injection about 12% of L209F-expressing oocytes whereas about 60% and 80% were alive in the calcium and cobalt containing media respectively. Figure 15 summarizes the effect of calcium and cobalt on oocyte viability. The strongest effect was observed with cobalt which boosted survival to 66 hours post-injection from 6% to 72%.

Conclusion

Overall the results suggest that L209F induces a calcium- and cobalt-sensitive leak current when expressed in oocytes. Membrane currents in L209F-expressing oocytes were several orders of magnitude greater than those of Cx31 and two other mutants. The leaky membranes were correlated with low survival of L209F-injected oocytes. Survival was enhanced by inclusion of 2 mM CaCl2 or 1 mM CoCl2 in the media surrounding the cells, consistent with aberrant hemichannel behavior. The effectiveness of calcium and cobalt in enhancing viability of L209F-expressing oocytes presents new avenues in the pursuit of therapeutic strategies in individuals suffering from

skin disease. Many questions remain including the question of whether Cx31L209F interacts with other connexins that are coexpressed in skin.

Figures

Figure 1

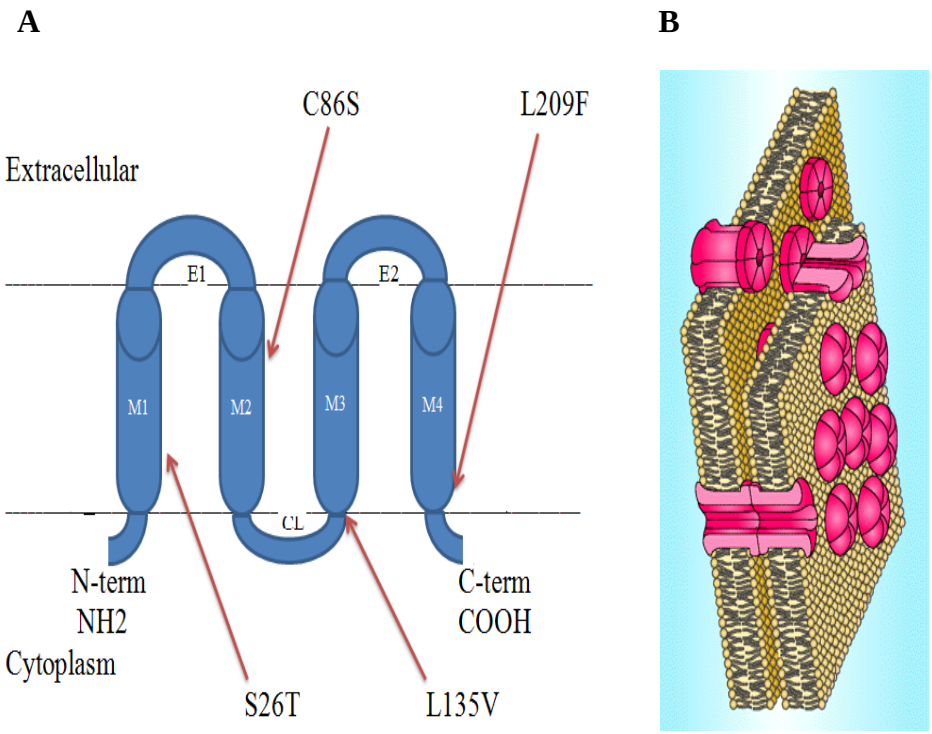

Figure 1. Connexin topology and gap junction organization. (A) Membrane topology of a typical connexin. Each connexin includes four transmembrane domains (M1-M4), two extracellular loops (E1and E2), a cytoplasmic loop (CL), and cytoplasmic amino and carboxyl domains. The location of mutations studied are indicated with arrows. (B) Gap junction channels are formed by the docking of two hemichannels (connexons), which together form a continuous aqueous pore linking the cytoplasm of the two cells. Each connexon is composed of six connexin proteins arranged around a central pore (Cook and Becker, 2009).

Figure 2

A **B**

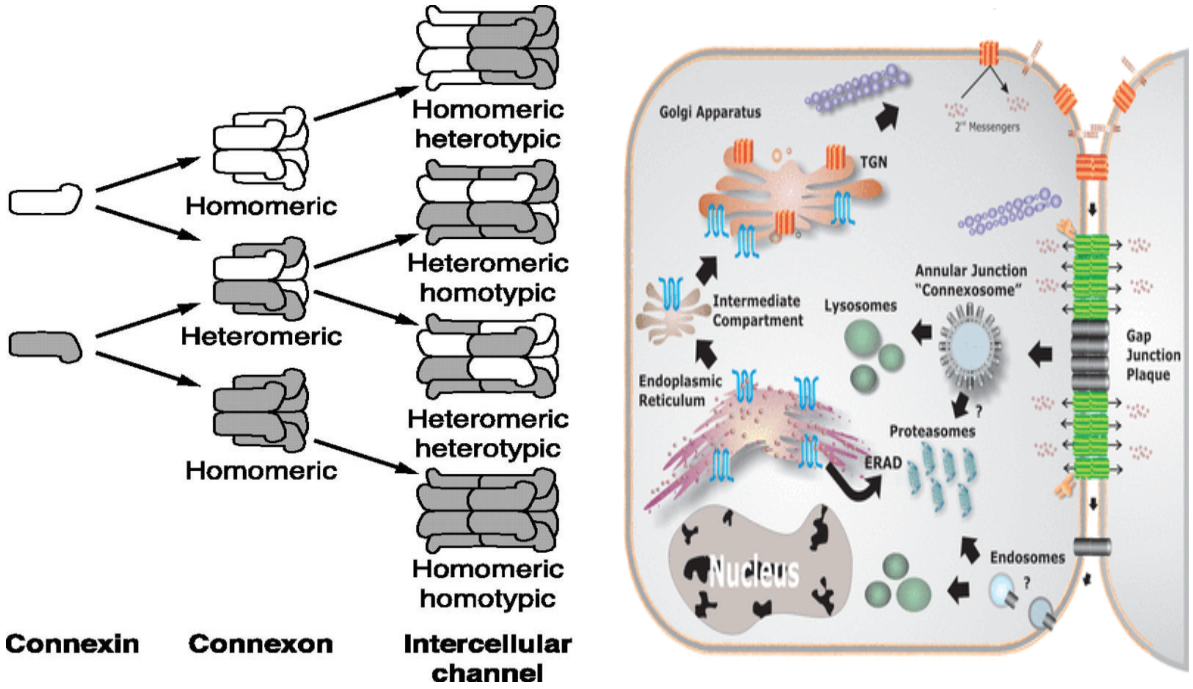

Figure 2. Cellular organization of connexins. (A) Arrangement of connexins into various channel types. Homomeric channels occur when one type of connexin makes up a connexon and heteromeric channels occur when different connexins make up a connexon. Docking of connexons results in either homotypic or heterotypic gap junction channels (Mathias *et al.*, 2010). (B) Connexin life cycle within a cell. A connexin protein begins its life cycle when it is cotranslationally inserted into the endoplasmic reticulum. On trafficking to the Golgi apparatus it undergoes oligomerization. After microtubule-facilitated transport to the cell surface, the connexon can dock with connexon counterparts from an adhered neighboring cell to form gap junction channels that aggregate with other channels constituting the mature gap junction or gap junction plaque (Laird, 2006).

Figure 3

A

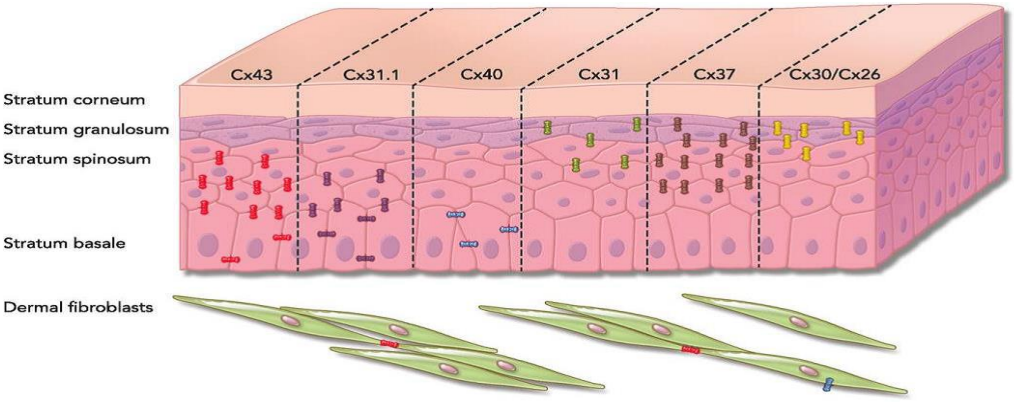

B

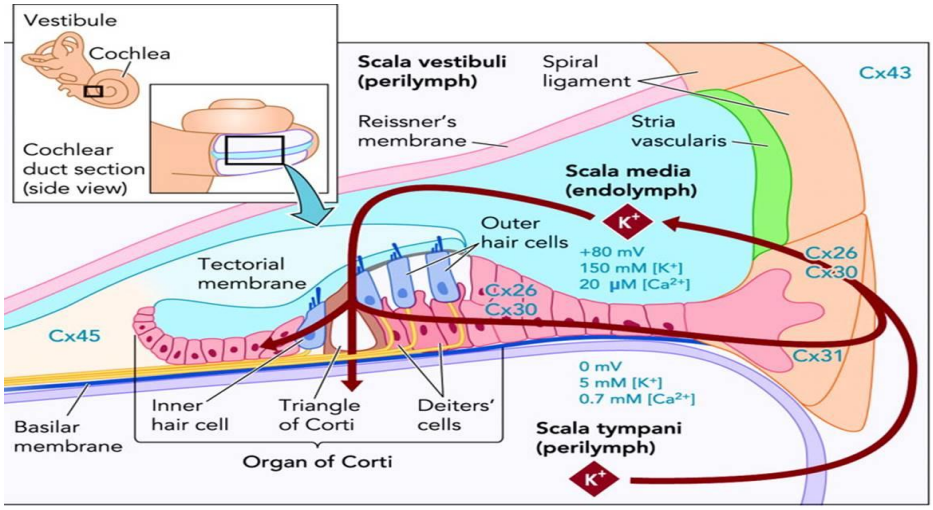

Figure 3. Organs where Cx31 is expressed (A) The epidermis is composed of four layers in thin skin: stratum basale, stratum spinosum, stratum granulosum, and stratum corneum. Several connexins are expressed in specific and overlapping patterns. Cx31 (green) is expressed in the statum granulosum and upper levels of the stratum spinulosum. Like Cx31, Cx37 (brown) is expressed in both the statum granulosum and stratum spinosum. Cx43 (red) and Cx31.1 (purple) are expressed in the stratum spinosum and stratum basale. Cx40 (blue) is restricted to the stratum basale. Cx30 and Cx26 (both in yellow) localize to various epidermal layers of epidermis (Churko and Laird, 2013). (B) Connexins are expressed in the inner ear where they play a role in development and distribution of potassium ions in the cochlea. Nonsensory epithelial cells indicated in pink express Cx26 and Cx30, while fibrocytes express Cx31 (Mammano *et al*., 2007).

Figure 4

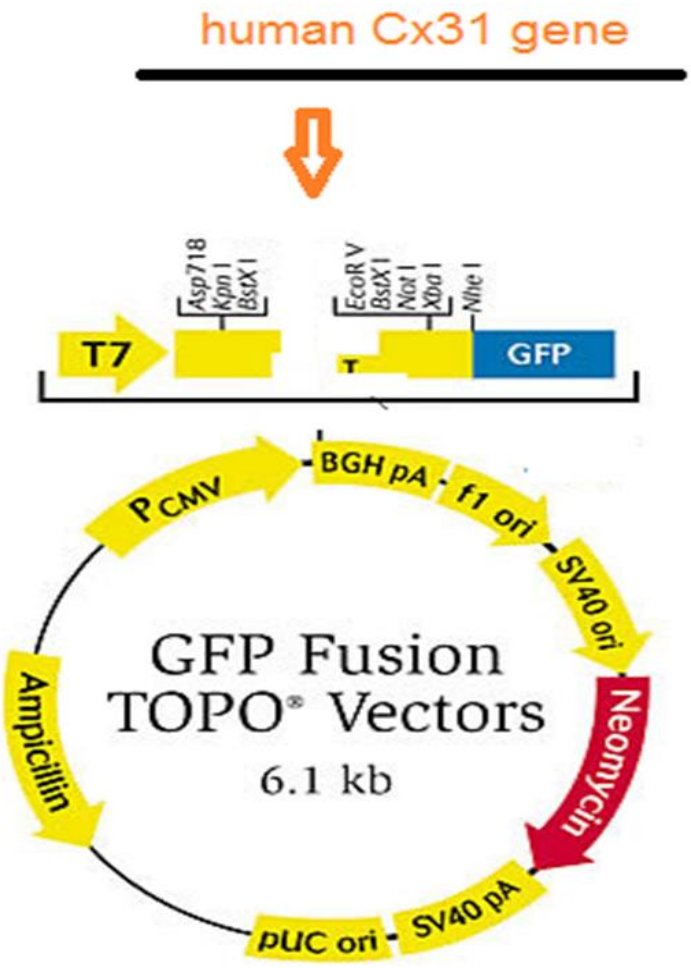

Figure 4. The gene encoding human Cx31 (GJB3) was inserted into a TOPO GFP fusion plasmid (*Thermoscientific, Grand Island NY*). The gene was inserted so that the T7 polymerase could be used to synthesize sense RNA. The Cx31 gene included a STOP codon and the GFP fusion did not occur. The GFP tag will be used for future studies involving expression in mammalian cell lines. The restriction enzyme *Xbal* was used to linearize the DNA prior to *in vitro* transcription.

Figure 5

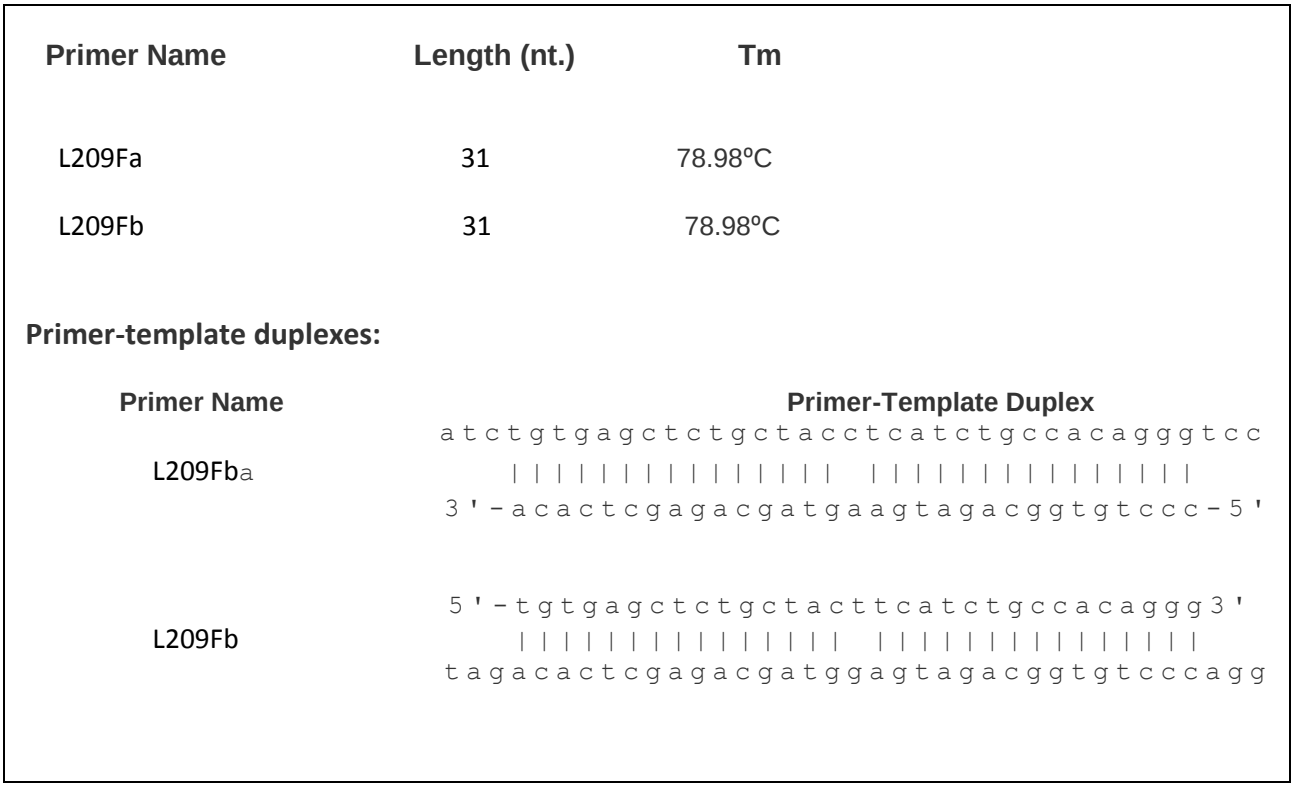

Figure 5. Using the Quikchange Primer Design Program on the s*tratagene.com website*, the human Cx31 gene sequence was modified to incorporate a mutation in the 209th codon resulting in the substitution L209F. Each primers is 31 bases in length with a Tm of 78.98^{0}C. The primers are complementary to one another to facilitate the mutation on opposite strands of the Cx31 sequence.

Figure 6

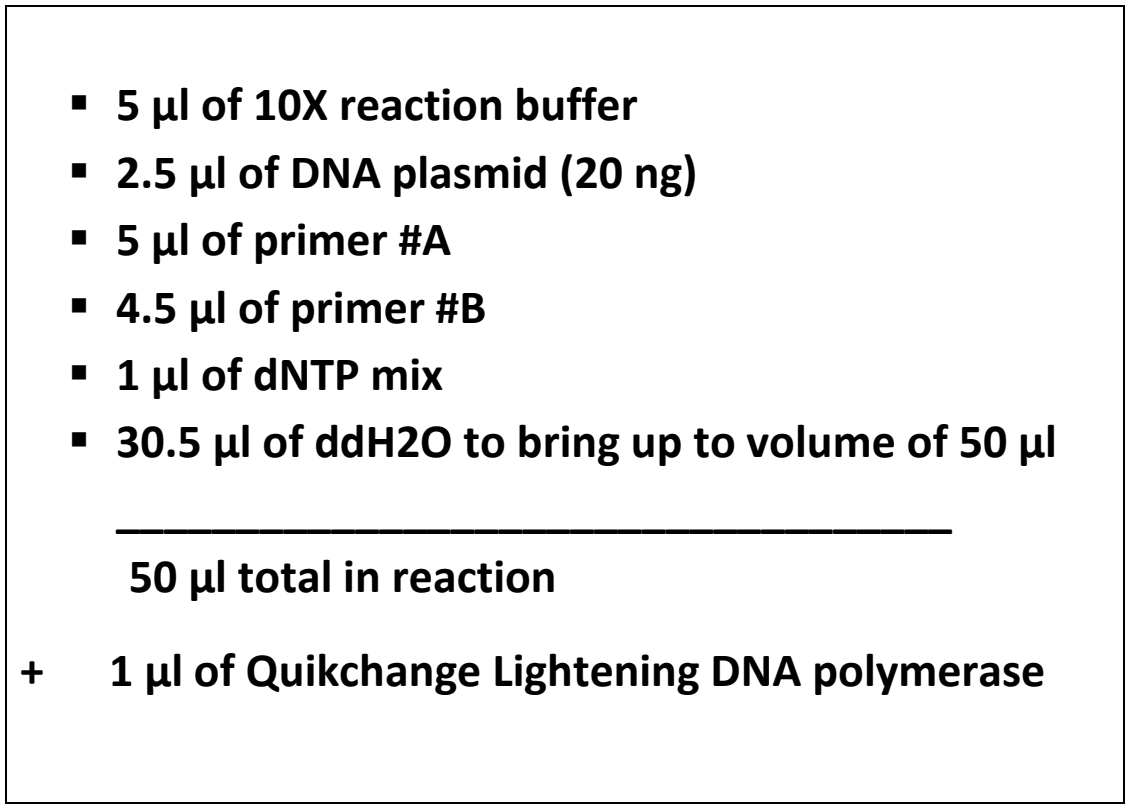

Figure 6. Components of the mutagenesis reaction. The reaction was assembled in a 500 µl thin-walled PCR tube in the order listed. One microliter of Quickchange lightening enzyme was added just prior to PCR.

Figure 7

Figure 7. Amino acid alignment of Cx31 (top) and the L209F mutant. The human Cx31 gene sequence was retrieved from Genbank (accession # gi 54607054) and translated using the "Sixframe" function on Biology Workbench (SanDiego Supercompter, SDSC). The mutant sequence was retrieved from Genscript (Piscataway, NJ) after plasmid DNA was sequenced in Genscript's sequencing facility. This sequence was translated using Sixframe and aligned with wildtype Cx31 amino acid sequence using ClustalW. Successful mutagenesis was confirmed by the change in leucine at position 209 to phenylalanine as indicated with the black box.

Figure 8

A

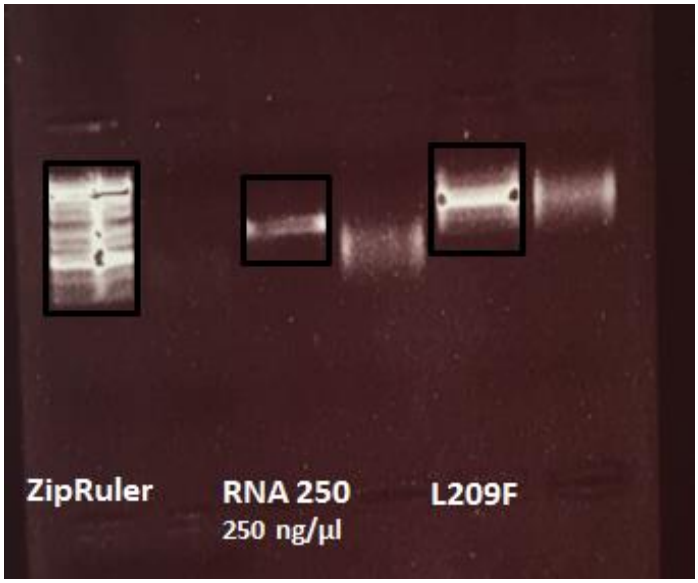

B

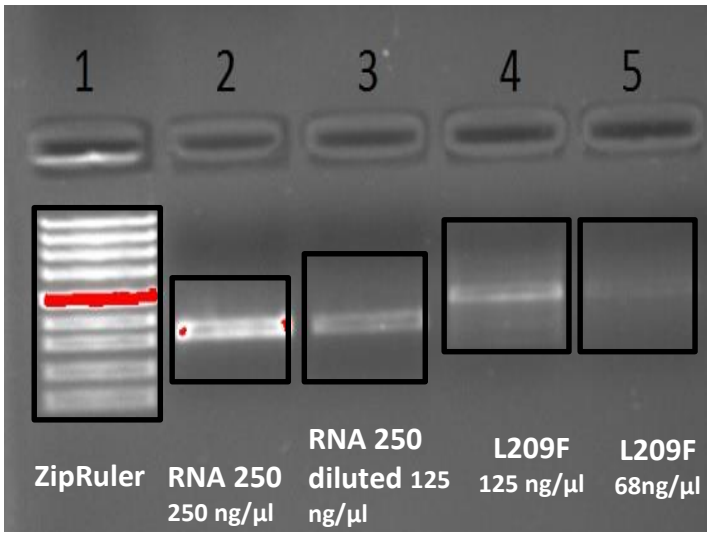

Figure 8. Examples of RNA analyzed by gel electrophoresis. Gels included 1% agarose in TAE and were run for approximately 20 minutes at 120V. (A) The *in vitro* transcription reaction for Cx31L209F was successful, generating about 1 µg/µl of RNA. (B) To assess the relationship between RNA and physiological effects of L209F, RNA was diluted. Diluting the RNA 250 CONTROL by half resulted in a decrease in band intensity (RNA 250 diluted to 125 ng/µl) which correlated well with the intensity of L209F (125 ng/µl). The subsequent dilution of L209F by one-half resulted in a further decrease in band intensity.

Figure 9

TMHMM predicted no change in TM4 topology as a result of phenylalanine substitution at position 209

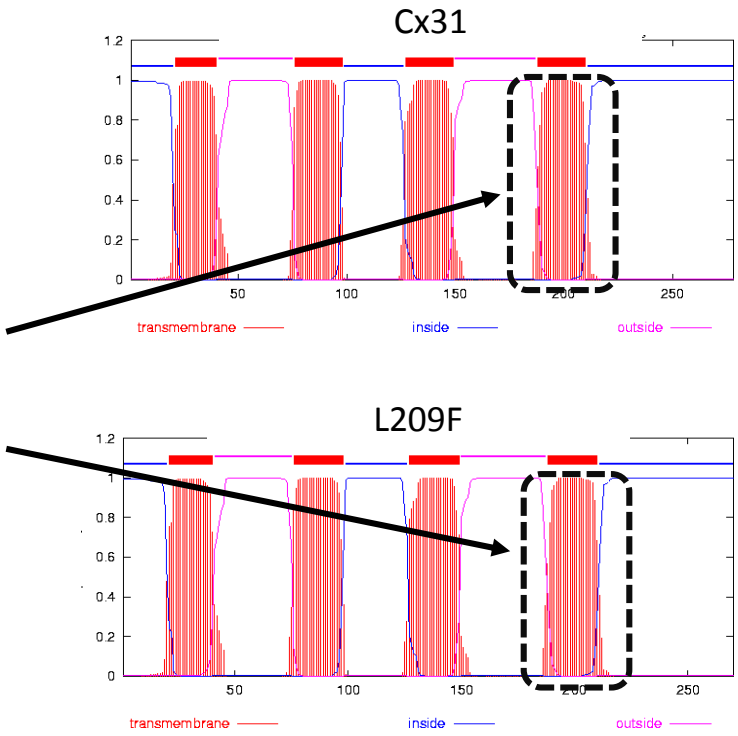

Figure 9. The membrane protein topology prediction program TMHMM (Krogh *et al.*, 2001) was used to assess potential changes in insertion of the fourth transmembrane domain due to the L209F substitution in Cx31. The program predicted that residues **188 through 210** span the lipid bilayer in both wtCx31 and Cx31L209F.

Figure 10

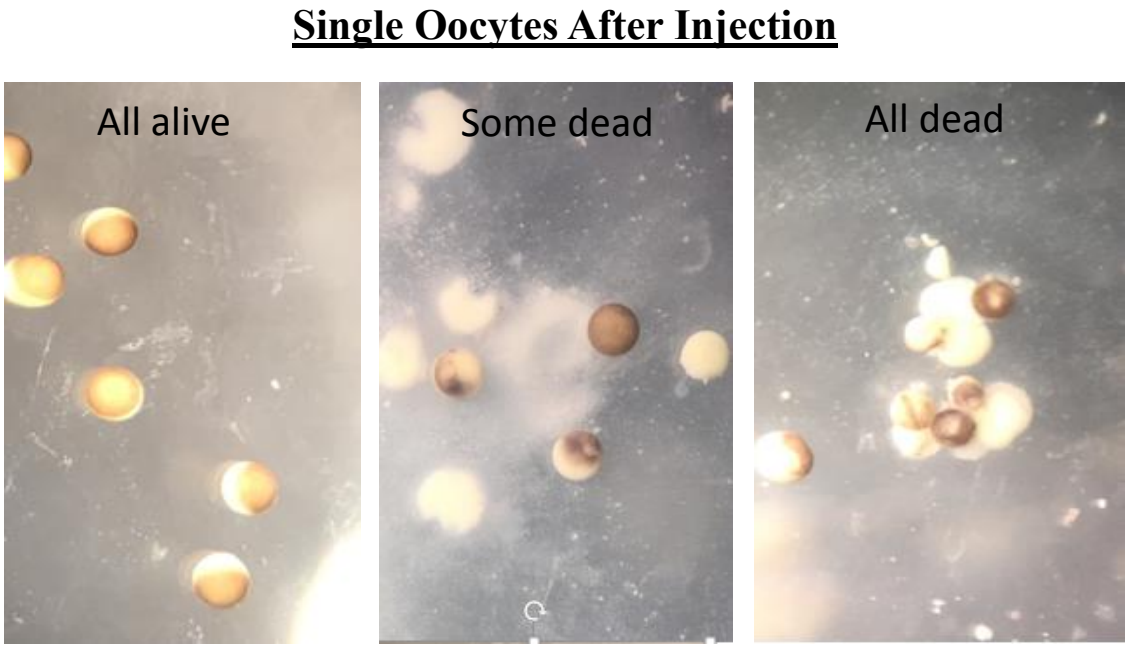

Figure 10. Images of *Xenopus* oocytes expressing connexins. Photographs were obtained using a typical digital camera through the lens of a dissecting microscope. Oocytes are about 1 mm in diameter. After injection with RNA encoding L209F, oocytes become turgid, the clear division between animal and vegetal pole was lost (center image, middle oocyte) and oocytes eventually progressed to bursting (right image). Once the oocytes burst the yolky cytoplasm is released into the surrounding media and often pools around the oocytes.

Figure 11

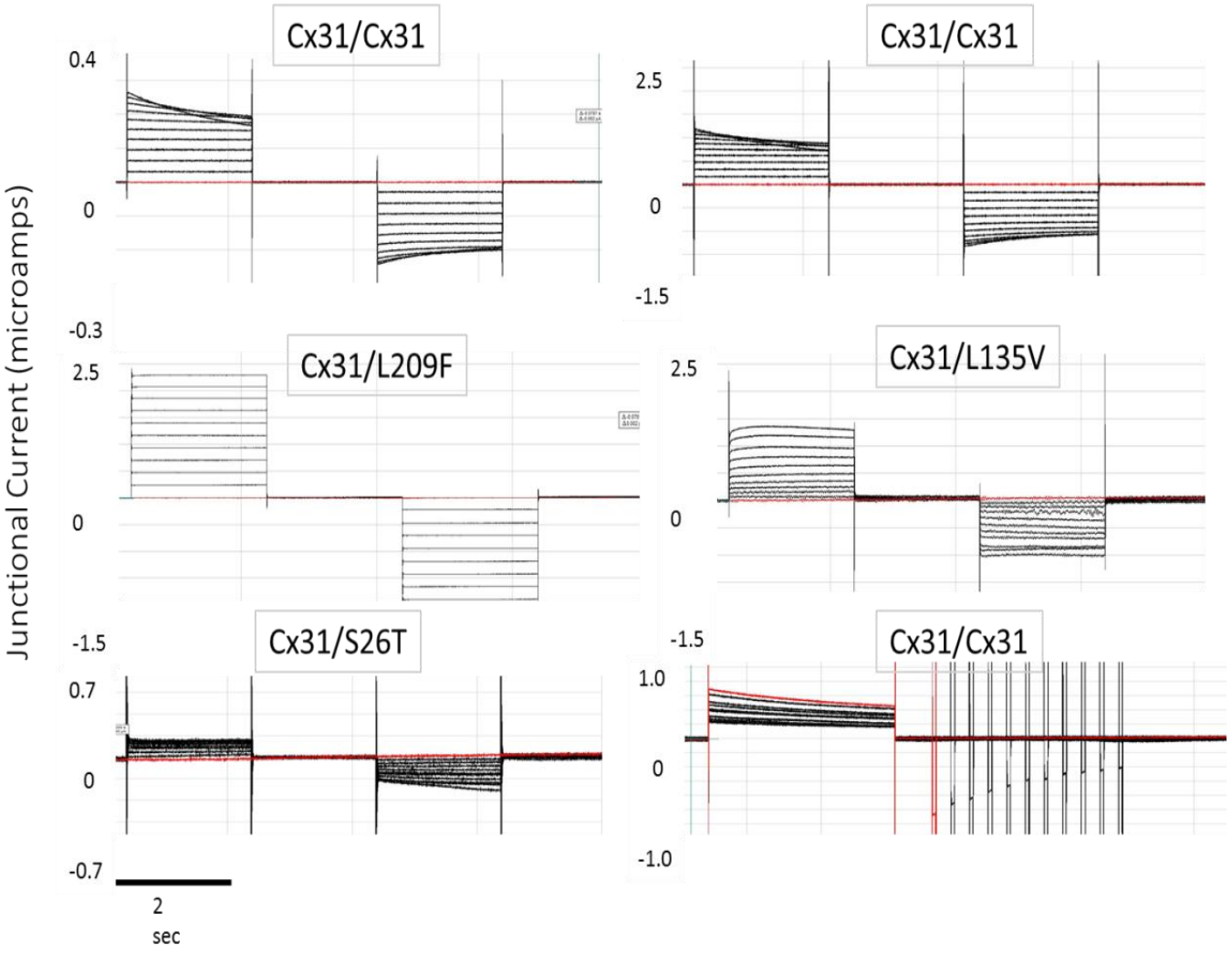

Figure 11. Gap junction currents recorded from paired oocytes expressing Cx31 and several skin disease mutants. For the first five sets of currents, cells were clamped at -20 mV and currents were recorded from this clamped cell while its partner was pulsed in 10 mV increments to induce transjunctional voltages (Vj's) between 100 mV and + 100 mV. In the last figure, recovery from inactivation was tested by repeatedly inducing a Vj of +100 mV for 4 seconds, followed by a variable recovery period and a short pulse to -100 mV.

Figure 12

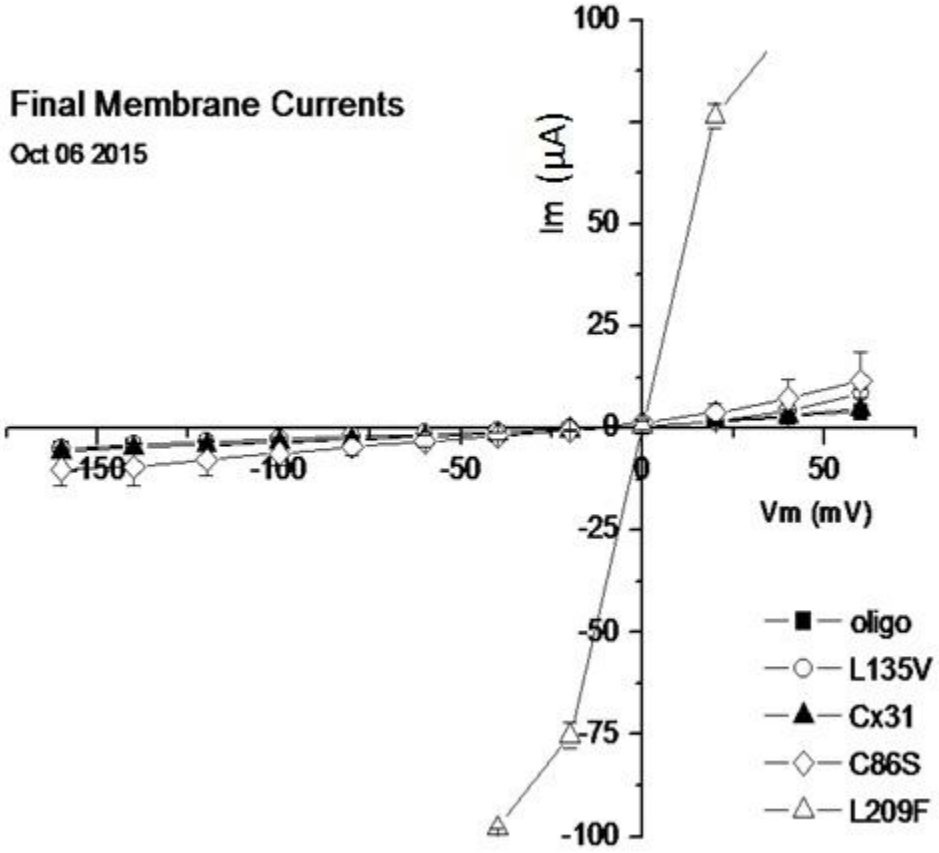

Figure 12. Membrane currents recorded in single oocytes expressing skin disease mutations Cx31 L135V, Cx31C86S and Cx31 L209F and oligo injected oocytes as a negative control. Oocytes were continuously clamped at -40 mV and pulsed in 20 mV increments to -140 and +40 mV. Voltage steps were 500 milliseconds in length and currents were measured at the end of the voltage pulse.

Figure 13

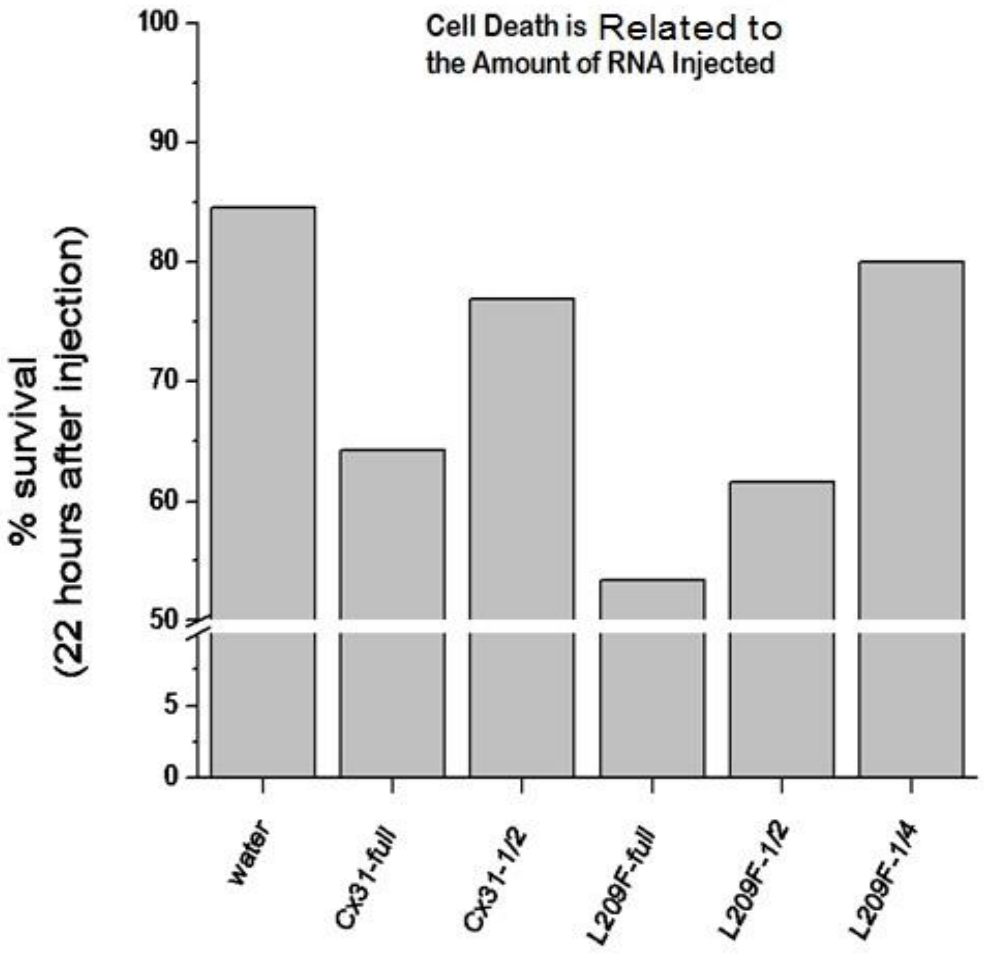

Figure 13. Survival of single oocytes injected with RNA encoding Cx31 or Cx31L209F. Full strength ≈ 125 ng/µl; ½ strength ≈ 68 ng/µl; ¼ strength ≈ 34 ng/µl.

Figure 14

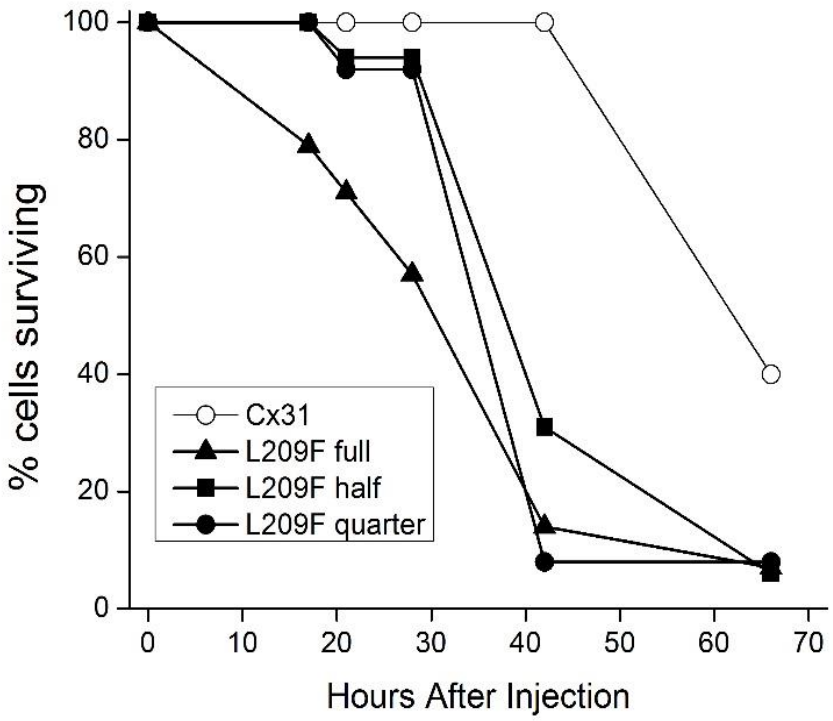

Figure 14. The Cx31 mutation L209F induces oocyte death in a time- and concentration-dependent manner. Oocytes were injected with either Cx31 RNA (125 ng/µl) or L209F FULL strength (125 ng/µl), HALF strength (68 ng/µl) or QUARTER strength (34 ng/µl). At each time point the number of surviving oocytes was counted and recorded.

Figure 15

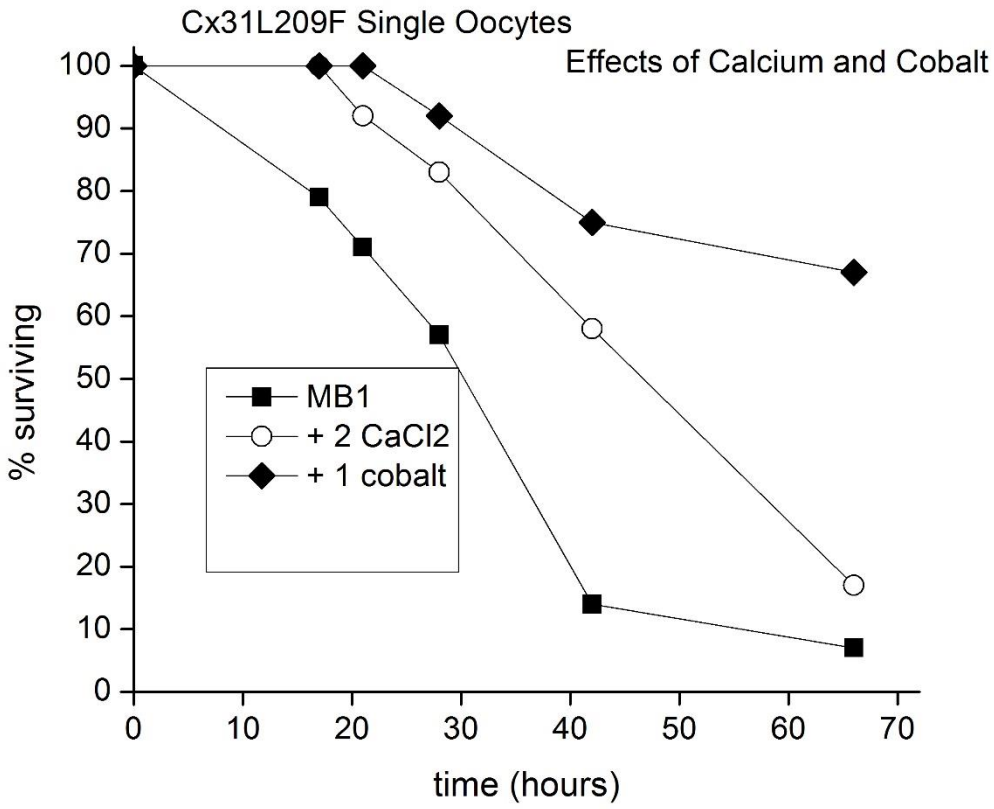

Figure 15. Viability of oocytes expressing the Cx31 mutation L209F is enhanced by calcium and cobalt. Oocytes were injected with either Cx31 RNA (125 ng/µl) or L209F RNA (125 ng/µl). Calcium (2 mM $CaCl_2$) and cobalt (1 mM $CoCl_2$) were added to the media immediately after injection. At each time point the number of surviving oocytes was counted and recorded.

References

Abrams CK, Freidin MM, Verselis VK, Bargiello TA, Kelsell DP, Richard G, Bennett MV, Bukauskas FF. 2006. Properties of human connexin 31, which is implicated in hereditary dermatological disease and deafness. Proc Natl Acad Sci USA 103: 5213-5218.

Alberts B, Johnson A, Lewis J, Raff M, Roberts K, and Walter P. 2005. Molecular Biology of the Cell. 5th Ed. Garland Sciences.

Brennan MJ, Karcz J, Vaughn NR, Woolwine-Cunningham Y, DePriest AD, Escalona Y, Perez-Acle T, Skerrett IM. 2015. Tryptophan Scanning Reveals Dense Packing of Connexin Transmembrane Domains in Gap Junction Channels Composed of Connexin32. J Biol Chem. 290: 17074-17084.

Churko JM, and Laird DW. 2013. Gap junction remodeling in skin repair following wounding and disease physiology. Physiol 28: 190-198.

Cook JE and Becker DL. 2009. Gap-Junction Proteins in Retinal Development: New Roles for the "Nexus". Physiol Rev 24: 219-230.

Dascal N. 1987. The use of Xenopus oocytes for the study of ion channels. CRC Crit Rev Biochem 22: 317-387.

Di WL, Rugg EL, Leigh IM, Kelsell DP. 2001. Multiple epidermal connexins are expressed in different keratinocyte subpopulations including connexin 31. J Invest Dermatol 117: 958–964.

Diestel S, Richard G, Döring B, Traub O. 2002. Expression of a connexin31 mutation causing erythrokeratodermia variabilis is lethal for HeLa cells. Biochem Biophys Res Commun. 296: 721-728.

Ebihara L. 2003. New roles for connexons. News Physiol Sci 18: 100-103.

Evans W H, Ahmad S, Diez J, George C H, Kendall J M, Martin PE. 1999. Trafficking pathways leading to the formation of gap junctions. Novartis Found. Symp 219: 44–54.

García IE, Maripillán J, Jara O, Ceriani R, Palacios-Muñoz A, Ramachandran J, Olivero P, Perez-Acle T, González C, Sáez JC, Contreras JE, Martínez AD. 2015. Keratitis-ichthyosis-deafness syndrome-associated Cx26 mutants produce nonfunctional gap junctions but hyperactive hemichannels when co-expressed with wild type Cx43. J Invest Dermatol 135: 1338-1347.

Goodenough DA and Paul DL (2009).Gap junctions. Cold Spring Harb Perspect Biol 1: a002576.

Gottfried I, Landau M, Glaser F, Di WL, Ophir J, Mevorah B, Ben-Tal N,Kelsell DP, Avraham KB. 2002. A mutation in GJB3 is associated with recessive erythrokeratodermia variabilis (EKV) and leads to defective trafficking of the connexin 31 protein. Hum Mol Genet 11: 1311–1316.

Harris AL. 2001. Emerging issues of connexin channels: biophysics fills the gap. Rev Biophys 34: 325-472.

He LQ, Liu Y, Cai F, Tan ZP, Pan Q, Liang D., Long ZG, Wu LQ, Huang LQ, Dai HP. 2005. Intracellular distribution, assembly and effect of disease-associated connexin 31 mutants in HeLa cells. Acta Biochim. Biophys 37: 547–554.

Itin P, Hohl D, Epstein EH Jr, DiGiovanna JJ, Compton JG, Bale SJ. 1998. Mutations in the human connexin gene GJB3 cause erythrokeratodermia variabilis. Nat Genet 20: 366-369.

Kadhim S. 2015. Expression and Characterization of Connexin31 Mutations Associated with Skin Disease and Deafness. Master's Thesis. Buffalo State College.

Kelsell DP, Dunlop J, Stevens HP, Lench NJ, Liang JN, Parry G, Mueller RF, Leigh IM. 1997. Connexin 26 mutations in hereditary non-syndromic sensorineural deafness. Nature 387: 80–83.

Kikuchi T, Adams JC, Miyabe Y, So E, Kobayashi T. 2000. Potassium ion recycling pathway via gap junction systems in the mammalian cochlea and its interruption in hereditary nonsyndromic deafness. Med Electron Microsc 33: 51-56.

Krogh A, Larsson B, von Heijne G, and Sonnhammer EL. 2001. Predicting transmembrane protein topology with a hidden Markov model: application to complete genomes. J Mol Biol 305: 567-580.

Kumar NM and Gilula NB. 1996. The gap junction communication channel. Cell 84: 381-388.

Laird DW. 2006. Life cycle of connexins in health and disease. Biochem J 394: 527–543.

Landowne D. 2006. Cell Physiology. LANGE Physiology Series. 1st Edition. McGraw Hill Companies, US.

Lilly E, Sellitto C, Milstone LM, White TW. 2016. Connexin channels in congenital skin disorders. Semin Cell Dev Biol 50: 4-12.

Lopez-Bigas N, Arbones ML, Estivill X, Simonneau L. 2002. Expression profiles of the connexin genes, Gjb1 and Gjb3, in the developing mouse cochlea. Gene Expr Patterns 2: 113–111.

López-Bigas N, Olive M, Rabionet R, Ben-David O, Martinez-Matos JA, Bravo O, Banchs I, Volpini V, Gasparini P, Avraham KB. 2001. Connexin 31 (GJB3) is expressed in the peripheral and auditory nerves and causes neuropathy and hearing impairment. Hum Mol Genet 10: 947–952.

Maeda S, Nakagawa S, Suga M, Yamashita E, Oshima A, Fujiyoshi Y, and Tsukihara T. (2009) Structure of the connexin 26 gap junction channel at 3.5A° resolution. Nature 458: 597-607.

Malchow RP, Qian H, Ripps H. 1993. Evidence for hemi-gap junctional channels in isolated horizontal cells of the skate retina. J Neurosci Res 35: 237-245.

Mall SR, Broadbridge R, Sharma RP, Lee AG, East JM. 2000. Effects of aromatic residues at the end of transmembrane α-helices on helix interactions with lipid bilayers. Biochem 39: 2071-2078.

Mammano F, Bortolozzi M, Ortolano S, and Anselmi F. 2007. Ca^{2+} Signaling in the Inner Ear. Physiol Rev 22: 131-144.

Martin PE, van Steensel M. 2015. Connexins and skin disease: insights into the role of beta connexins in skin homeostasis. Cell Tissue Res 360: 645-658.

Mathias RT, White TW, and Gong X. 2010. Lens Gap Junctions in Growth, Differentiation, and Homeostasis. Physiol Rev 90: 176-206.

Morley SM, White Mi, Rogers M, Wasserman D, Ratajczak P, McLean WH, Richard G. 2005. A new, recurrent mutation of GJB3, Cx31, in erythrokeratoderma variabilis. Br J Dermatol 152: 1143-1148.

Musil LS and Goodenough DA. 1993. Multisubunit assembly of an integral plasma membrane channel protein, gap junction connexin43, occurs after exit from the ER. Cell 74: 1065–1077.

Oh SK, Choi SY, Yu SH, Lee KY, Hong JH, Hur SW, Kim SJ, Jeon CJ, Kim UK. 2013. Evaluation of the pathogenicity of GJB3 and GJB6 variants associated with nonsyndromic hearing loss. Biochim Biophys Acta.1832: 285-291.

Phelan P. 2005. Innexins: Members of an evolutionarily conserved family of gap-junction proteins. Biochim Biophys Acta 1711: 225–245.

Rouan F, Lo CW, Fertala A, Wahl M, Jost M, Rodeck U, Uitto J, Richard G. 2003. Divergent effects of two sequence variants of GJB3 (G12D and R32W) on the function of connexin 31 *in vitro*. Exp Dermatol 12: 191-197.

Richard G, Smith LE, Bailey RA, Itin P, Hohl D, Epstein EH Jr, DiGiovanna JJ, Compton JG, Bale SJ. 1998. Mutations in the human connexin gene GJB3cause erythrokeratodermia variabilis. Nat Genet 20: 366-369.

Richard G, Brown N, Smith LE, Terrinoni A, Melino G, Mackie RM, Bale SJ, Uitto J. 2000. The spectrum of mutations in erythrokeratodermias--novel and de novo mutations in GJB3. Hum Genet 106: 321-329.

Saez JC, Retamal MA, Basilio D, Bukauskas FF, and Bennett MV. 2005. Connexin-based gap junction hemichannels: gating mechanisms. Biochim Biophys Acta 1711: 215–224.

Scott CA, and Kelsell DP. 2011. Key Function for Gap Junctions in Skin and Hearing. Biochem J 438: 245-254.

Scott CA, O'Toole EA, Mohungoo MJ, Messenger A, Kelsell DP. 2011. Novel and recurrent connexin 30.3 and connexin 31 mutations associated with erythrokeratoderma variabilis. Clin Exp Dermatol 36: 88-90.

Skerrett IM, Smith JA, and Nicholson BJ. 1999. Mechanistic Differences Between Chemical and Electrical Gating of Gap Junctions In: Current Topics in Membranes. Volume 49. Ed. C. Peracchia Academic Press, CA. pp 249-269.

Skerrett IM, Di WL, Kasperek EM, Kelsell DP, Nicholson BJ. 2004. Aberrant gating, but a normal expression pattern, underlies the recessive phenotype of the deafness mutant Connexin26M34T. FASEB J 18: 860-862.

Tattersall D, Scott CA, Gray C, Zicha D, Kelsell DP. 2009. EKV mutant connexin 31 associated cell death is mediated by ER stress. Hum Mol Genet 18: 4734-4745.
Unsworth HC, Aasen T, McElwaine S, and Kelsell DP. 2007. Tissue-specific effects of wild-type and mutant connexin 31: a role in neurite outgrowth. Hum Mol Genet 16: 165–172.

Verselis VK, Ginter CS, Bargiello TA. 1994. Opposite voltage gating polarities of two closely related connexins. Nature 368: 348-351.

Verselis VK, Trelles MP, Rubinos C, Bargiello TA, Srinivas M. 2009. Loop gating of connexin hemichannels involves movement of pore-lining residues in the first extracellular loop domain. J Biol Chem 284: 4484-4493.

Werner R, Miller T, Azarnia R, Dahl G. 1985. Translation and functional expression of cell-cell channel mRNA in Xenopus oocytes. J Memb Biol 87: 253-268.

Willecke K, Eiberger J, Degen J, Eckardt D, Romualdi A, Güldenagel M, Deutsch U, Söhl G. 2002. Structural and functional diversity of connexin genes in the mouse and human genome. Biol Chem 383: 725-737.